OPTIMIZATION OF VERTICAL ROTARY TILLAGE BLADE PARAMETERS FOR SALINE-ALKALI LAND IMPROVEMENT

/

面向盐碱地改良的立式旋耕刀结构参数优化

Xuan LUO, He SUN, Haoran BAI*)
College of Mechanical and Electrical Engineering, Qingdao Agricultural University Qingdao /China
Tel: +86 13854285625; E-mail: baihaoran111@126.com
Corresponding author: Haoran BAI
DOI: https://doi.org/10.35633/inmateh-76-101

Keywords: *saline–alkali land, vertical rotary tiller blades, tool speed ratio, discrete element method, soil fragmentation, tillage simulation*

ABSTRACT

To address the limitations of conventional tillage machinery in compacted, high–viscosity saline–alkali lands, this study designed a vertical rotary tiller tool structure suitable for deep fragmentation operations in saline-alkali lands, aiming to improve soil fragmentation efficiency and reduce operational resistance. Employing orthogonal experiments and response surface methodology (RSM), this study established a quadratic regression model correlating soil fragmentation rate and blade force, utilizing the tool camber angle, blade inclination angle, and internal bending angle as key variables. On this basis, a kinematic model of the cutting tool was constructed, and the correlation between the speed ratio and operating conditions was elucidated. Based on the EDEM simulation platform, the dynamic characteristics of cutting force, torque, particle flow velocity, and particle force during one complete rotation of the cutting tool in saline–alkali land were simulated and analyzed. Results indicated that the tool camber angle and internal bending angle exerted the most significant influence on operational effectiveness, with a notable interaction effect observed between them. An optimal parameter combination was ultimately derived through optimization: camber angle of 8.06°, blade–inclination angle of 7.48°, internal bending angle of 7.46°, resulting in a force of 2295.27 N and a soil fragmentation rate of 91.59%. The results established a theoretical foundation for optimizing vertical tiller blade design, while practical guidance for saline-alkali land tillage was developed through studies on soil fragmentation and energy use.

摘要

针对盐碱地土壤板结严重、黏重性高等特点导致传统耕整机械适应性差的问题，本文设计了一种适用于盐碱地深层破碎作业的立式旋耕机刀具结构，旨在提高碎土率和降低作业阻力。研究选取刀具外倾角、刀刃倾角和内折弯角作为主要影响因素，结合正交试验与响应面分析方法，建立了碎土率和刀具受力的二次回归模型。在此基础上，构建刀具运动学模型，明确了速度比与作业工况之间的匹配关系。基于 EDEM 仿真平台，模拟分析刀具在盐碱地中旋转一周内的受力、扭矩、颗粒流速与颗粒力的动态变化特性。结果表明，刀具外倾角和内折弯角对作业性能影响显著，且二者间存在交互作用。优化结果显示，当外倾角为 8.06°、刀刃倾角 7.48°、内折弯角为 7.46° 时，刀具受力为 2295.27 N，碎土率为 91.59%。研究为立式旋耕刀具的结构优化提供了理论依据，并通过碎土率和能耗特性的研究，为改善盐碱地机械化整地作业质量提供了实践指导。

INTRODUCTION

China possesses diverse land resource types, yet high–quality cultivated land is relatively scarce. Saline–alkali land accounts for over 10% of the total cultivated land area in the country. According to statistics from the National Plan for Saline-Alkali Land Resource Utilization (2021–2030), more than 100 million mu (approximately 6.67 million hectares) of saline-alkali land nationwide is available for development, characterized by wide distribution and significant potential *(Chang et al., 2025)*. However, saline–alkali lands are universally characterized by high soil hardness, severe compaction, and elevated viscosity, which result in increased operational resistance and poor soil fragmentation when conventional tillage machinery was employed, severely constraining reclamation efficiency. The amelioration of saline–alkali lands has been recognized as a critical measure for enhancing agricultural productivity and ensuring food security.

In recent years, multiple techniques, including biological, chemical, physical, and integrated agronomic approaches have been explored through research and practical applications *(Vlăduţoiu et al., 2017; Popescu et al., 2022)*.

Among these, the development of high–efficiency tillage equipment adapted to saline–alkali land conditions was identified as a vital pathway for improving operational efficiency and reclamation outcomes. Concurrently, relevant studies provided methodological and theoretical references from the perspectives of machinery selection, structural optimization, and soil–tool interaction mechanisms *(Ungureanu et al., 2015; Vlăduţ et al., 2017)*.

In the mechanized reclamation of saline-alkali lands, rotary tillage equipment was widely adopted due to its demonstrated capabilities in soil fragmentation and cultivation layer improvement. As a new type of tillage machinery, the vertical rotary tiller breaks up the soil structure from multiple angles after the blades cut vertically into the soil, making it more suitable for deep soil compaction improvement than traditional horizontal rotary tillers. Meanwhile, its detailed working effect, uniform tillage layer, low energy consumption, and strong adaptability have made it one of the important technical directions for the mechanized improvement of saline-alkali land *(Fang et al., 2016; Zhang et al., 2013)*. However, most existing vertical rotary tillers are designed for general use, and their blade structures have not been systematically optimized for the complex soil conditions of saline-alkali land, which limits further improvements in their operational performance.

In response to this issue, some scholars have conducted research on tool structure optimization. *Yang et al. (2025)* analyzed the impact of the outward tilt angle on the force distribution and operational quality of the Sangyuan power harrow, while *Wang et al. (2019)* optimized the operational parameters of the vertical-driven shallow rotary harrow based on tool kinematics and dynamics. These studies provide references for the optimization of vertical rotary tillage tools; however, there remains a gap in specialized adaptive design tailored for saline-alkali soils. Therefore, this paper aims to improve saline–alkali land by designing a vertical rotary tillage tool adapted to saline-alkali land working environments, establishing a cutting kinematic model, analyzing the impact of structural parameters on operational performance, and selecting the optimal parameter combinations that reduce power consumption and improve operational quality through discrete element simulation and field trials, thereby providing a theoretical basis and technical support for the efficient mechanized improvement of saline-alkali land *(Ucgul et al., 2020; Makange et al., 2021)*.

MATERIALS AND METHODS

Vertical rotary tiller structure design and working principle

The cutter assembly functions as the working component of the vertical rotary tiller, making direct contact with the soil. The blades are mounted vertically and rotate about individual axes. The implement performance depends on cutting tool characteristics, and the cutter assembly was 3D–modeled in SolidWorks 2022, with its full structure shown in Figure 1.

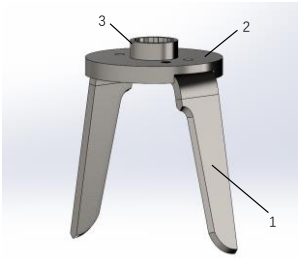

Fig. 1 –Diagram of the cutter assembly structure

1 - Tool; 2 - Base; 3 - Tool axis

The rake knife on the rotor has a swivel diameter of 240 mm (material: 65Mn steel), and the thickness of the non-cutting area at the front end is designed to be 7 mm to ensure the structural strength of the cutting edge. To avoid cutter assembly interference and missed plowing, the width of the cutter assembly is 90 mm, the length is 60 mm, and the thickness is 15 mm, in accordance with the size of the cutter disc and the installation distance between the rotors. Considering the characteristics of saline-alkali land with serious soil compaction and a deeper plowing layer, the plowing depth needs to reach 200–250 mm, so the total height of the tool is set to 300 mm, of which the length of the cutting edge is 260 mm (Fig. 2).

The structural parameters of the cutting tool are designed as follows: α is the camber angle of the cutting tool, which affects its working coverage area. By adjusting the camber angle, the overlap rate between rotors can be optimized, effectively preventing leakage and improving the uniformity of soil fragmentation, thereby enhancing operational efficiency and controlling energy consumption.

β is the blade–inclined angle, which affects the soil penetration performance of the cutting tool. A larger inclination angle helps reduce soil penetration resistance but may decrease the soil contact area, thereby affecting the effectiveness of soil fragmentation. Therefore, its value must be balanced according to actual soil conditions. γ is the internal bending angle, which plays a key role in the dynamic performance of the cutting tool. Without an internal bending angle, the back of the cutter in contact with the soil is prone to the phenomenon of "anti-soil," which increases operating resistance and machine vibration.

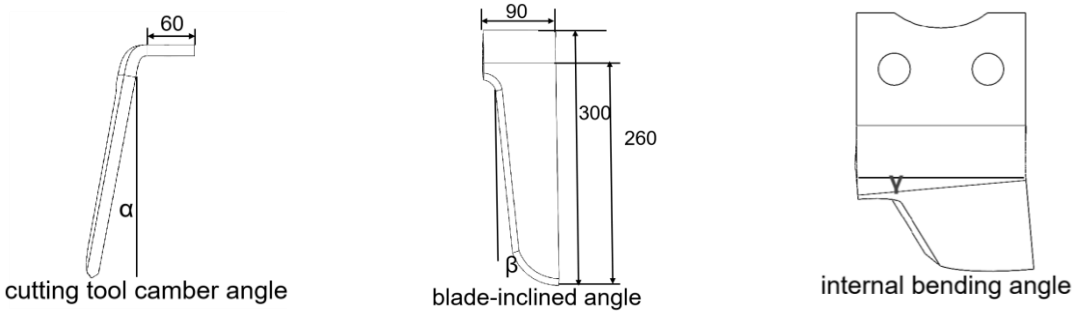

(a) Main view *(b) Side view* *(c) Top view*

Fig. 2 – Schematic diagram of the cutting tool structure

Kinematic analysis of soil cutting

The trajectory of the blade at any point is depicted in Figure 3. The cutter movement of the vertical rotary tiller consists of two parts: one is the linear movement that advances with the whole machine, and the other was the circular rotary movement around its own axis, and the two are superimposed to form a spiral ground–cutting path.

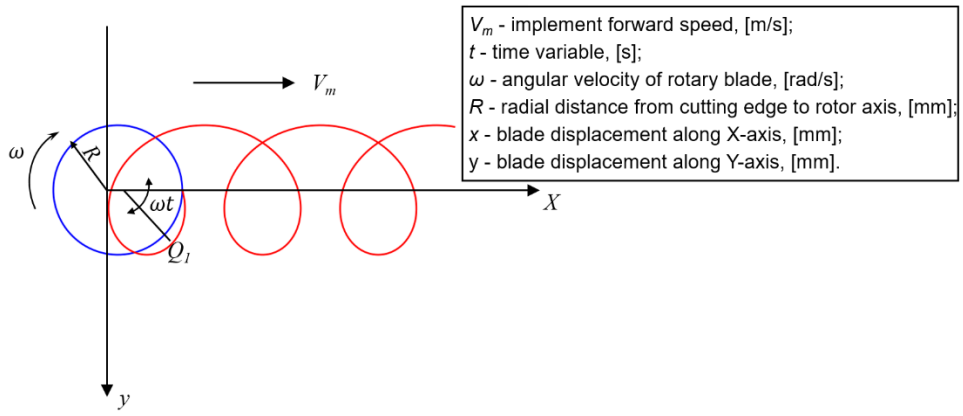

Fig. 3 – Diagram of the cutting tool motion trajectory

The kinematic trajectory of the blade tip after time t was described by the following Equations (1-2):

$$x = R\cos\omega t + V_m \text{ t} \quad (1)$$

$$y = -R\sin\omega t \quad (2)$$

The tool speed ratio λ is defined as the ratio of the implement forward velocity V_m to the product of the blade rotational angular velocity ω and the cutting radius R. Set the tool speed ratio Equation (3):

$$\lambda = \frac{\omega R}{V_m} \quad (3)$$

The angular velocity Equation (4) is:

$$\theta = \omega t \quad (4)$$

Substituting λ and θ yields:

$$x = R\left(\frac{\lambda}{\theta} + cos\theta\right) \quad (5)$$

$$y = -Rsin\theta \quad (6)$$

where:

V_m is the implement forward speed, [m/s];

t – time variable, [s];

ω – angular velocity of rotary blade, [rad/s];

R – radial distance from cutting edge to rotor axis, [mm];

x – blade displacement along X-axis, [mm];

y – blade displacement along Y-axis, [mm];

θ – angle, [°];

λ – tool speed ratio.

From this, the motion trajectory was a pendulum motion. Equations (1–2) were analyzed using Python. The simulation parameters comprised: (1) cutting edge radius R = 110 mm (rotor axis to blade tip, (2) operational conditions with V_m = 1 m/s forward speed the rotary cutter and three rotational velocities (0.5,1, and 1.5 rev/s), and (3) temporal domain limited to t = 1 s. The three motion trajectories are shown in Figure 4.

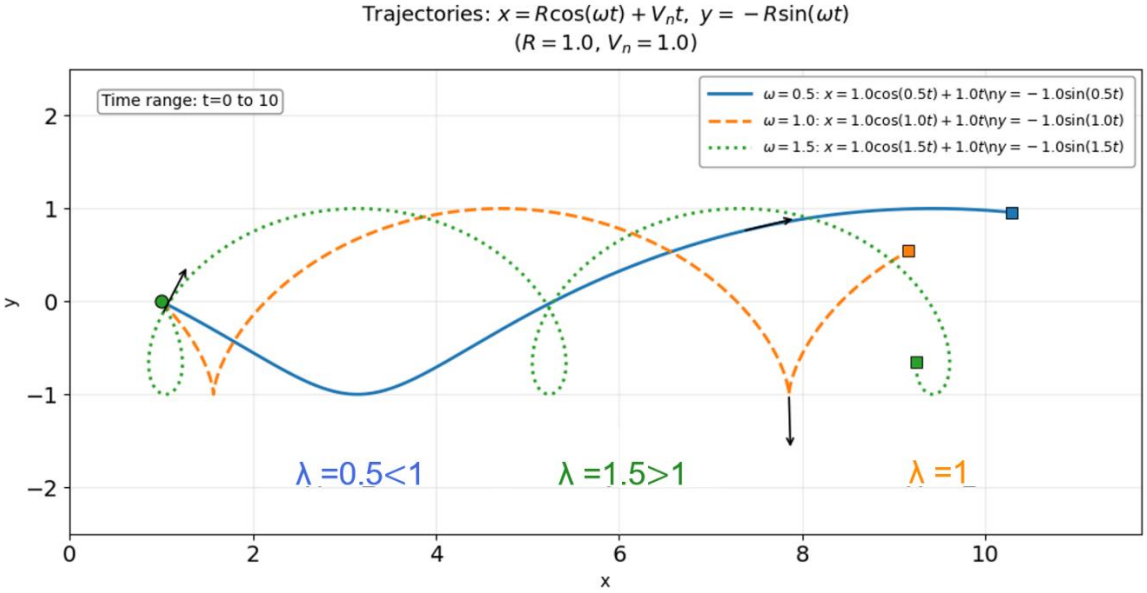

Fig. 4 – Three types of motion trajectory diagrams

When λ < 1, the trajectory is a short pendulum and the blade plays a role in pushing the soil.

When λ = 1, the trajectory is a standard pendulum and the blade plays a role in piercing the soil.

When λ > 1, the trajectory is a long pendulum line, the blade plays a role in crushing the soil.

Therefore, λ >1, the vertical tiller normal operation of the sufficient conditions, the rotational speed of the tool should be greater than the forward speed of the tiller.

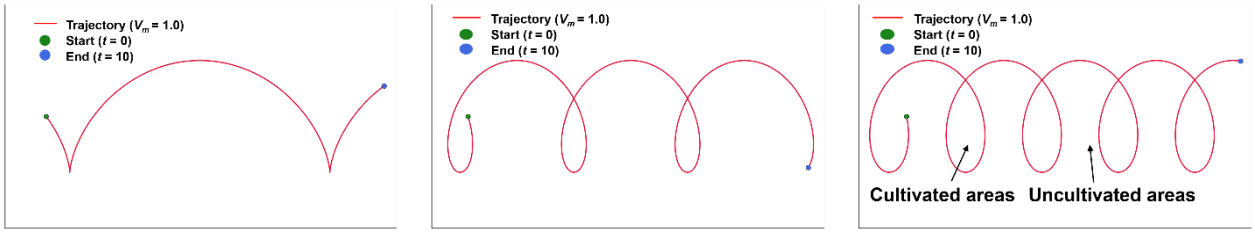

(a) λ=1 *(b) λ=2* *(c) λ=3*

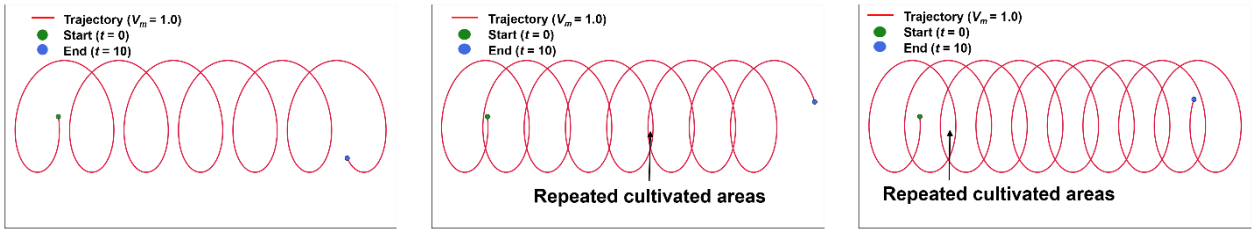

(d) λ=4 *(e) λ=5* *(f) λ=6*

Fig. 5 – Motion trajectory under different speed ratios

Figure 5 shows that as λ increased, the overlapping area of the harrow blade movement trajectory line increases, which means that as λ increases, the plowed area increases and the unplowed area decreases. When λ > 4, the area of repeated plowing appeared. To avoid unnecessary power consumption, the structure, power consumption and productivity of the vertical rotary tiller should be considered, and the value range of λ should be 1 < λ < 4.

Simulation based on EDEM

Soil modeling

With notable variations in particle size, shape, and physical characteristics, soil was a highly heterogeneous discrete particle medium. To facilitate simulation modeling and improve computational efficiency, this paper simplifies soil particles using smooth solid spheres to approximate the unit particles. Spherical particles not only simplify contact calculations but also effectively enhance simulation stability.

In discrete element simulations, the choice of particle size directly affects the computational load and simulation accuracy. The number of contact calculations decreases with larger particle sizes while the simulation speed increases, but this results in a less accurate description of the actual soil details. Considering the balance between simulation accuracy and efficiency, the radius of soil particles in the EDEM software was set to 5 mm in EDEM 2022 software, allowing the simulation model to better reflect the mechanical response of real soil.

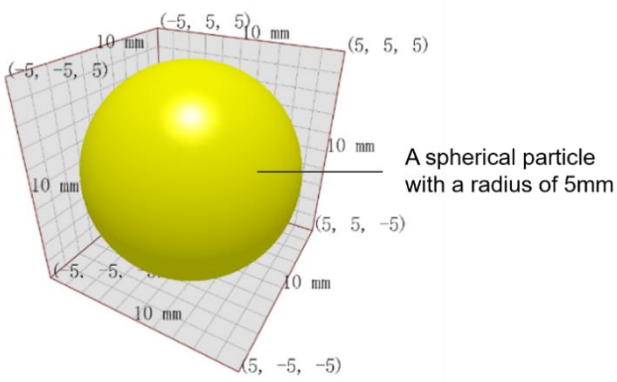

Fig. 6 – Particle model

To accurately describe the interactions between soil particles and between particles and tools, the Hertz–Mindlin with JKR model and the Hertz–Mindlin with Bonding model were chosen as particle contact models. The Hertz–Mindlin with JKR model was mainly used to describe the nonlinear elastic contact behavior with adhesion, suitable for the bonding phenomenon between fine particles caused by surface energy, especially under saline–alkali land conditions. Its contact force included three components: elastic force, damping force, and adhesive force. To further simulate the fragmentation process of soil structures under external forces, the Hertz–Mindlin with Bonding model was introduced. Based on the basic elastic contact, the "bonding bond" was added in this model, which broke after meeting certain fracture criteria to simulate the rupture of soil aggregates. This model could accurately reflect the process of soil evolving from a clustered state to a discrete state when disturbed by a tool, thereby accurately predicting the soil fragmentation effect *(Ucgul et al., 2018; Sun et al., 2018)*.

Simulation parameter setting

Soil test samples were taken from the saline-alkali agricultural trial demonstration base in the Yellow Delta Agricultural Highland Zone, Dongying City, Shandong Province, with a pH value of 8.2. By reviewing the relevant literature *(Wang et al., 2024)*, the specific parameters of the discrete meta-simulation were determined as shown in Table 1.

Table 1

Setting of simulation parameters of soil model

Project	Property	Unit	Parameter Value
Soil particles	Poisson's ratio		0.32
	Shear module	Pa	1.2×10^{8}
	Density	kg/m^3	2270
Blade	Poisson's ratio		0.3
	Shear module	Pa	7.9×10^{10}
	Density	kg/m^3	7865
Soil particles-rake knife	Coefficient of restitution		0.3
	Static friction factor		0.5
	Kinetic friction factor		0.1
Soil particles-soil particles	Coefficient of restitution		0.358
	Static friction factor		0.546
	Kinetic friction factor		0.15
Soil JKR surface energy		J/m^2	3.207

Construction of soil tank model and simulation process

A three–dimensional model of vertical rotary tiller blades was developed using SolidWorks 2022 software and exported in the STL file format. The model was subsequently imported into EDEM 2022 software, where a complete simulation system was established to conduct operational simulations of the vertical rotary tillage tools. Considering that during actual vertical tiller operation, adjacent blades had to employ identical rotational speeds but opposite rotational directions to maintain operational stability, two tillage blades were configured as a functional group in the simulation model for modeling and analytical purposes. According to the simulation of actual saline soil cultivation conditions, considering the actual working size and the influence of the simulation boundary, the length of the soil tank was set to 1200 mm, the width of the soil tank at 1000 mm, and the height of the soil tank to 400 mm. The simulation process of the vertical rotary tiller was shown in Figure 7. Based on previous kinematic analysis of soil cutting, the simulation parameters were set to a 1.2 m/s forward speed, 4 r/s rotational speed and 250 mm working depth for plow pan disruption in saline–alkali lands. The total duration of the simulation was set to 12 s, during which the soil particles were arranged according to the random filling mode in 0–10 s, and the natural accumulation was accomplished by gravity settling to ensure the reasonable distribution of the particles and the contact stability to meet the requirements of the initial simulation conditions. The vertical rotary tillage blade was used for normal rotary tillage operation in 10–12 s.

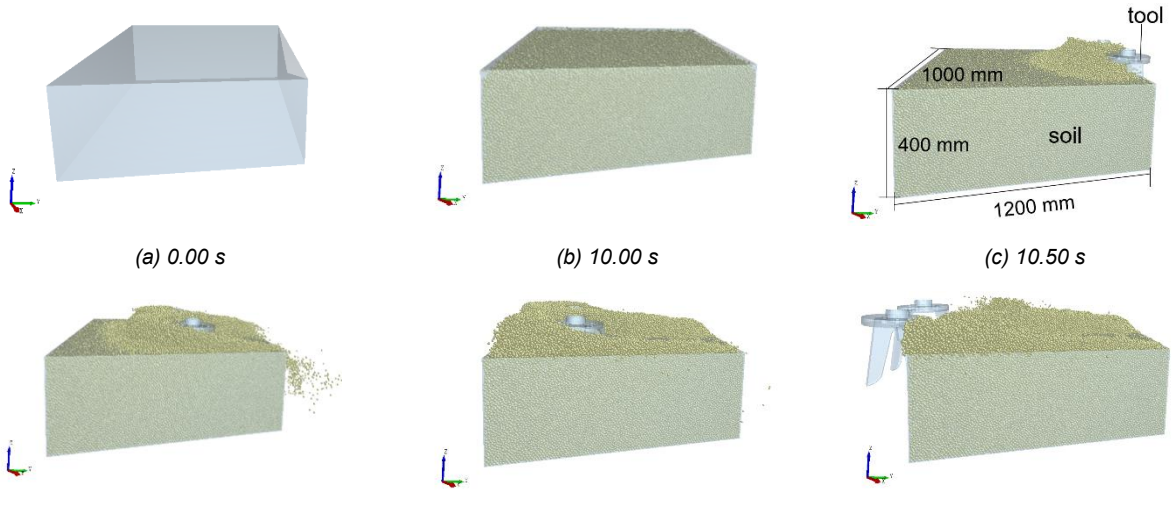

(a) 0.00 s *(b) 10.00 s* *(c) 10.50 s*

(d) 11.00 s *(e)11.50 s* *(f) 12.00 s*

Fig. 7 – Simulation process of a vertical rotary tiller

RESULTS AND DISCUSSIONS

Analysis of force and torque variations in rotary tillage tools

To thoroughly investigate the force characteristics and soil response during vertical rotary tillage operations in saline-alkali soils, dynamic simulation analysis was conducted on the total tool force, torque, particle flow velocity, and particle force over a complete rotation cycle. By comparing the mechanical responses between two consecutive cycles (10.60–11.10 s), the periodic patterns and synergistic effects during tool-soil interaction were examined, revealing the influence of high cohesion and aggregation properties of saline-alkali lands on particle motion transmission and energy dissipation, which provides theoretical guidance for tool structural optimization and operational parameter matching. As depicted in Figures 8 and 9, distinct periodic fluctuations in tool force were observed during the 10.6–11.1 s interval, with each complete rotation corresponding to one full cycle of force variation. Specifically, the first rotational cycle (10.60–10.85 s) was characterized by multiple peaks and troughs in both force and torque curves, indicating significant load variations when cutting through soils of different compaction levels. The second cycle (10.85–11.10 s) exhibited essentially identical fluctuation patterns to the first, confirming stable tool-soil interaction characteristics. Based on these findings, subsequent orthogonal experiments could be performed using single-cycle simulations to conserve computational resources.

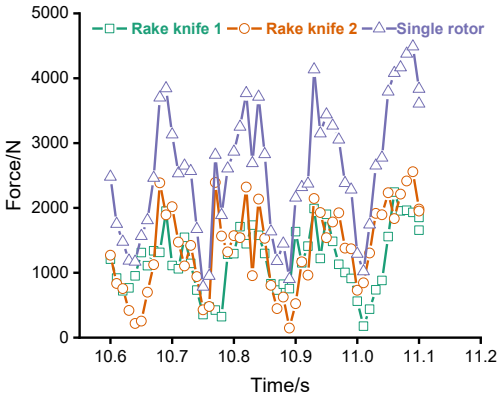

Fig. 8 – Curve of force versus time

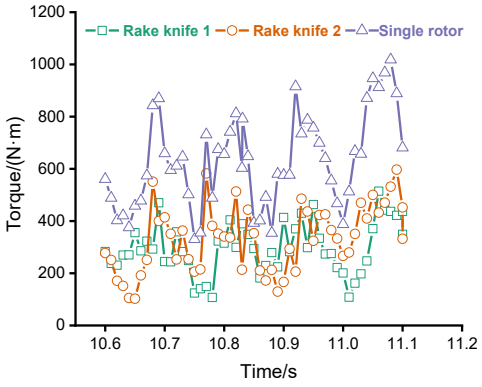

Fig. 9 – Curve of torque versus time

Trends in particle flow rate and particle force

During tool rotation, the dynamic response of soil perturbation was reflected through concurrent variations in particle flow velocity and particle force. Analysis of two complete rotational cycles (10.60–11.10 s) demonstrated high temporal synchronization between these parameters (Fig. 10 and Fig. 11).

The overall trend indicated that after soil engagement and incision by the tool, particle force underwent rapid intensification, resulting in elevated particle flow velocity; upon progressive tool retraction from the active zone, particle force and flow velocity exhibited a synchronous decrease, manifesting characteristic cyclic variation. In the first cycle (10.60–10.85 s), the particle flow velocity and force reached a trough around 10.64 s, followed by a synchronized rapid increase to a local peak with a flow velocity of 0.1845 m/s and particle force of 0.0847 N around 10.70 s, indicating that at this time, the depth of tool penetration and the soil reaction force were synchronously enhanced. In the second cycle (10.85–11.10 s), the two continued to maintain synergistic fluctuations, indicating that the perturbation rhythm had a certain regularity.

As the saline-alkali soil had the characteristics of high cohesion and strong agglomeration, which made the cohesion between particles larger in the disturbance process, the particle flow rate enhancement lagged the force enhancement, and the damping effect in the particle movement process was more obvious. The rigid characteristics of the soil structure led to the fluctuation of particle force before and after the peak value being larger than the fluctuation of flow rate, reflecting the influence of saline soil structure on the particle motion transfer process.

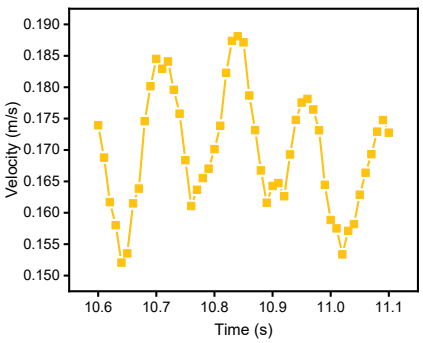

Fig. 10 – Curve of velocity versus time

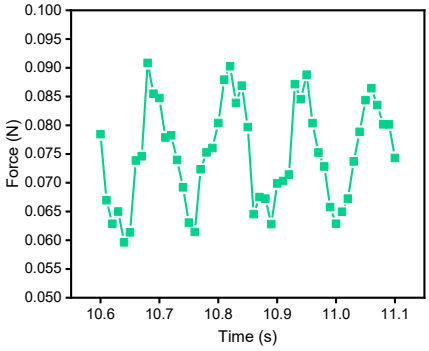

Fig.11 – Curve of force versus time

Results of the multi-factor experiments

An investigation into the effects of tool camber, blade–inclined, and internal bending angles on soil crushing rate and force distribution was conducted employing the orthogonal test methodology; response surface methodology was subsequently applied to establish quantitative relationships between these structural parameters and tillage performance through mathematical modeling; finally, a three–factor, three–level orthogonal experiment was conducted to identify the key influencing factors through significance analysis and optimize the tool parameter combination. From the previous trend of force and torque changes, it was observed that the fluctuation of the tool's force and torque in each motion cycle was smooth, so the following orthogonal test only needed to perform the simulation process of one motion cycle *(Chen et al., 2025)*. The factor levels of the test tool were displayed in Table 2, and the test results were shown in Table 3.

Table 2

Simulation test factors and levels

Encodings	Tool camber angle A	Blade-inclined angle B	Internal bending angle C
a	0	0	0
b	5	5	5
c	10	10	10

Table 3

Structural parameter results and analysis of vertical rotary tiller

Standards	Tool camber angle	Blade-inclined angle	Internal bending angle	Force	Soil fracture rate
1	b	b	b	2294.33	91.92
2	c	b	c	2231.12	91.12
3	c	a	b	2300.14	89.25
4	a	c	b	2478.65	90.76
5	c	b	a	2390.56	89.32
6	b	b	b	2310.52	91.71
7	b	a	a	2543.75	88.52
8	b	b	b	2305.20	91.45
9	b	c	c	2270.65	90.42
10	b	b	b	2280.64	91.72
11	a	b	c	2300.68	92.65
12	b	a	c	2269.50	93.50
13	a	b	a	2612.25	91.25

Standards	Tool camber angle	Blade-inclined angle	Internal bending angle	Force	Soil fracture rate
14	b	c	a	2425.65	90.45
15	b	b	b	2285.68	91.14
16	a	a	b	2601.25	92.56
17	c	c	b	2386.10	87.50

Regression modeling and response surface analysis of forces were performed using Design–expert 13.0 software. Quadratic regression analysis was done on the tillage resistance of vertical rotary tiller to obtain the response surface regression model.

$$F=2295.27-85.61A-112.53C+52.15AB+38.03AC+76.27A^2+70.00B^2 \quad (7)$$

As can be seen from Table 3, the regression model between the vertical rotary tiller forces and the test factors was highly significant (P < 0.01), indicating that the model was able to explain the force variations well. The out-of-fit term was not significant (P=0.0799 > 0.01), suggesting that the model fits well and can be used for prediction. The results showed that the combined effect of tool camber, blade-inclined, and internal bending angle were the main factors affecting the force on vertical rotary tiller, followed by blade-inclined, and there was a significant interaction between the factors.

Table 4

ANOVA of the force regression model

Source	Sum of squares	Freedom	Mean of squares	F-value	P-value	Significance
Model	2.325×10^5	9	25829.33	60.82	＜0.0001	Significant
A	58630.86	1	58630.86	138.05	＜0.0001	
B	2947.20	1	2947.20	6.94	0.0337	
C	1.013×10^5	1	10.013×10^5	238.53	＜0.0001	
AB	10878.49	1	10878.49	25.61	0.0015	
AC	5785.88	1	5785.88	13.62	0.0077	
BC	3555.14	1	3555.14	8.37	0.0232	
A^2	24491.82	1	24491.82	57.67	0.0001	
B^2	20633.35	1	20633.35	48.58	0.0002	
C^2	617.53	1	617.53	1.45	0.2671	
Residual	2973.01	7	424.72			
Lack of fit	2334.95	3	778.32	4.88	0.0799	Insignificant
Pure Error	638.06	4	159.51			
Cor Total	2.354×10^5	16				

Note: P<0.01 (indicates highly significant);

Regression modeling and response surface analysis of soil fracture rate using Design–expert 13.0 software. A quadratic regression analysis was done on the soil fragmentation rate of vertical rotary tiller to obtain a response surface regression model.

$$W=91.59-1.25A+1.02C-1.25BC-0.9640B^2 \quad (8)$$

Table 5

Analysis of variance for regression modeling of soil fracture rate

Source	Sum of squares	Freedom	Mean of squares	F-value	P-value	Significance
Model	35.59	9	3.95	10.46	0.0027	Significant
A	12.53	1	12.53	33.13	0.0007	

Source	Sum of squares	Freedom	Mean of squares	F-value	P-value	Significance
B	2.74	1	2.74	7.24	0.0310	
C	8.30	1	8.30	21.96	0.0022	
AB	0.0012	1	0.0012	0.0032	0.9562	
AC	0.0400	1	0.0400	0.1058	0.7545	
BC	6.28	1	6.28	16.60	0.0047	
A^2	1.52	1	1.52	4.03	0.0847	
B^2	3.91	1	3.91	10.35	0.0147	
C^2	0.0409	1	0.0409	0.1080	0.7520	
Residual	2.65	7	0.3781			
Lack of fit	2.28	3	0.7615	8.41	0.0335	Insignificant
Pure Error	0.3623	4	0.0906			
Cor Total	38.24	16				

Note: P<0.01 (indicates highly significant);

As shown in Table 5, the model of the relationship between the soil fracture rate of the vertical rotary tiller and the test factors was highly significant (P < 0.01), indicating the model could explain the soil fracture rate well. Meanwhile, the lack-of-fit term was not significant (P=0.0335 > 0.01), suggesting the model was well fitted. This proved the modified model was superior and could be used for prediction. The results showed that under the combined effect of tool camber, blade–inclined angle, and internal bending angle, tool camber and internal bending angle had the most significant effect on the soil fracture rate, followed by blade-inclined.

Influence of interaction factors on operational effectiveness

The force response surface was shown in Figure 12. Both the contact area at the tool-material interface and resultant force direction were determined by blade-inclined angle, while force distribution pattern and transmission pathway were governed by tool camber angle. The surface shape reflected their interaction: the peak area indicated significant force trend change under specific combinations, caused by superposition of contact area and force distribution. Internal bending angles affected tool rigidity and cutting path, with contour distribution revealing its greater sensitivity to force effects compared to tool camber angle. It directly altered cutting edge effective length and stress concentration degree. Cutting edge geometry and material removal mechanisms were jointly influenced by internal bending angle and tool camber. The surface trend demonstrated that blade-inclined increased with internal bending angle, cooperatively changing cutting edge entry angle and material deformation zone distribution.

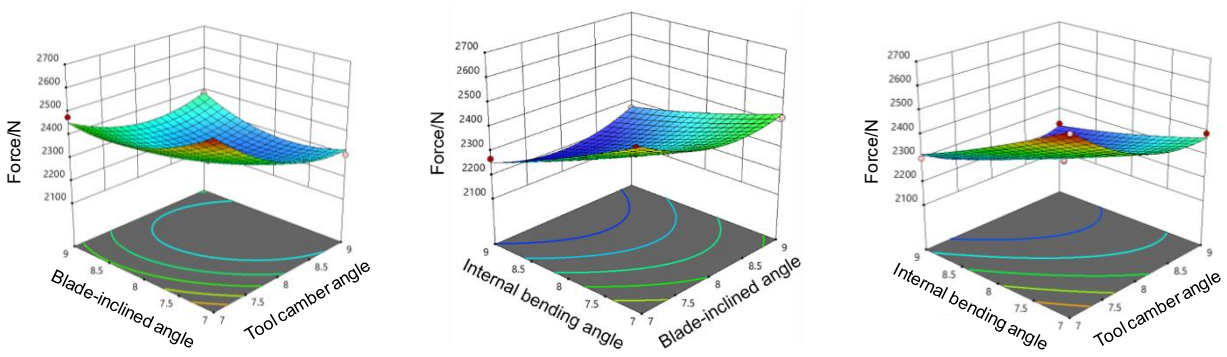

(a) AB *(b) BC* *(c) AC*

Fig. 12 –The surface on which the interaction responds to the force

A - Tool camber angle; B -Blade-inclined angle; C - Internal bending angle; AB - The impact of A and B on force; AC - The impact of A and C on force; BC - The impact of B and C on force

The soil fracturing rate response surface was shown in Figure 13. The contact angle between cutting edge and soil was determined by blade-inclined angle, influencing soil crushing efficiency. The tool camber angle altered lateral cutting–edge distribution, modifying soil crushing coverage. The surface showed higher soil fragmentation in the middle region, indicating parameter interaction. The shear crushing effect on soil was directly influenced by blade-inclined angle, while lateral soil extrusion and crushing range were affected by tool camber angle. The aggregation and crushing paths of the tool on soil were affected by internal bending angle, with crushing rate first increasing then decreasing as internal bending angles increased. With tool camber angle variation, small internal bending angles exhibited crushing rate constrained by camber angle, whereas near peak areas demonstrated enhanced parameter interaction jointly determining crushing rate improvement. Soil breakage rate sensitivity to tool camber response increased with internal bending angle.

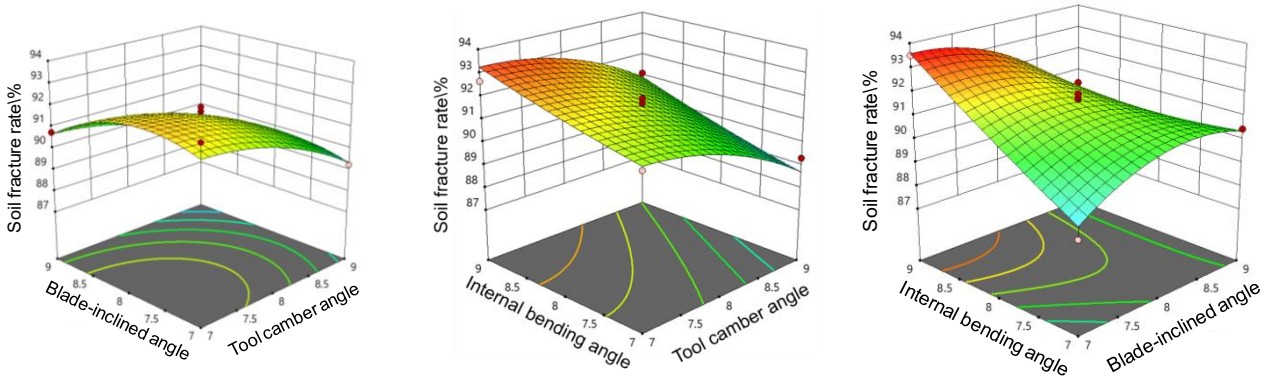

(a) AB *(b) AC* *(c) BC*

Fig. 13 – Response surfaces for the effect of interaction terms on the soil fracture rate

A - Tool camber angle; B - Blade-inclined angle; C - Internal bending angle; AB - The impact of A and B on force; AC - The impact of A and C on force; BC - The impact of B and C on force

In order to obtain the optimal combination of operating parameters of vertical rotary tiller, two regression models were optimized and solved by using the Numerical module of Design–Expert 13.0 software. In saline-alkali land, the force of vertical rotary tiller was 2295.27 and the soil breakage rate was 91.59% with the tool camber angle of 8.06°, the tool camber angle of 7.48°, and the internal bending angle of 7.46°.

Field trial

To validate the field performance of the simulation–optimized structural parameters of the vertical rotary tiller blades in saline–alkali soil conditions, field tests were conducted to validate the optimized vertical rotary tiller performance in saline-alkali lands at the Yellow River Delta Agricultural High-tech Zone, Dongying City, Shandong Province.

Fig. 14 – Field trial process

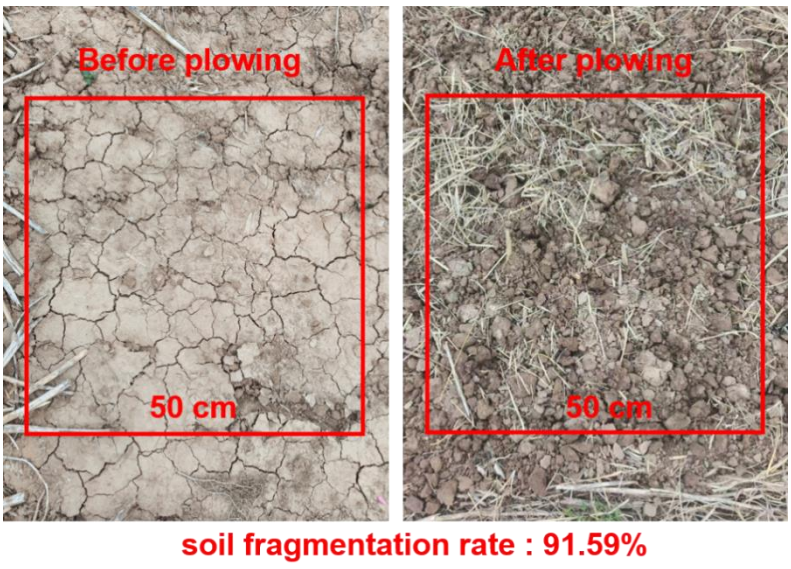

Fig. 15 – Field trial effect

A Deutz–Fahr 1804 tractor was used with 1.2 m/s forward speed and 240 rpm blade rotation. The experimental site was characterized by moderate saline-alkali soil with severe surface compaction, unimplemented spring tillage, and flat terrain (50 m length × 10 m width). The cultivated layer exhibited significant soil hardness *(Gao et al., 2023; Zhang et al., 2024; Qin et al., 2016)*. The measurement equipment included: an electronic balance (maximum capacity: 2500 g, accuracy: 0.1 g), a steel tape measure (range: 5 m, accuracy: 0.1 cm), and a steel ruler (range: 50 cm, accuracy: 0.5 mm). The tests were performed in mid-March 2025 under clear weather conditions, following identical experimental protocols as previously described.

The tests were conducted to validate the simulation optimization combinations (external inclination angle of 8.06°, blade–inclined angle of 7.48°, and internal bending angle of 7.46°), respectively, and the evaluation index was the soil fragmentation rate. In the test area, a 50 × 50 cm area was taken every 5 m in a trip (3 areas in total) and a 50 × 50 cm self-made frame was placed. At the same time, the soil quality of the cultivated layer and the soil block quality greater than 4 cm in the frame were weighed, and the soil fragmentation rate of the 3 areas was calculated respectively, and the average value was obtained *(Xiao et al., 2024; Ucgul et al., 2017*).

The soil fragmentation rate can be obtained from Equation (9):

$$F = \frac{M_t - M_d}{M_t} \times 100\% \quad (9)$$

where:

F is the soil fragmentation rate, [%];

M_t – the mass of all the soils, [g];

M_d - the mass of the soil block with the longest length larger than 4 cm, [g].

Table 6

Validation test results

Test conditions	Soil fracture rate (%)
1	88.55
2	89.14
3	90.21
Average value	89.30
Predicted value	91.59
Mean relative error/%	2.29

The results suggested that the soil fracture rate of the optimized structural combination reached 91.59%, and the results of the field validation test were shown in Table 7, which showed that the soil fracture rate after the test was 89.30%, and the mean relative error of the average value was 2.29% compared with the results of the simulation test, which might be due to the fact that the vibration of the machine in the actual operation process led to a lower soil fracture efficiency than that of the simulation test. However, the deviation was in line with the simulation and actual error range, so it could be considered that the simulation test results were basically consistent with the field test results. The knives had no obvious wear and tear or grass tangling phenomenon under continuous operation conditions, and the operation stability was excellent.

Comprehensive analysis indicated that the simulation-optimized tool structure not only performed well in the discrete element simulation, but also had the characteristics of high soil crushing efficiency, low energy consumption, and high adaptability in the actual saline-alkali land operation, which verified the engineering feasibility and practicability of the simulation and the response surface optimization model, providing theoretical and practical support for the subsequent product promotion and mechanized operation.

CONCLUSIONS

This paper focused on the application requirements of vertical rotary tiller in saline–alkali land improvement operation and carried out the research on optimization of blade structure parameters and simulation analysis of operation performance. By establishing the kinematic model of the tool, the relationship between the tool speed ratio and the operating quality was clarified, which provided a theoretical basis for the reasonable determination of the operating parameters.

Based on EDEM discrete element simulation software, Hertz-Mindlin with JKR and Bonding contact model was adopted to establish a soil simulation system for saline land cultivation. The simulation results demonstrated that the vertical rotary tiller blades exhibited significant periodic fluctuations in both force and torque during operation, with highly consistent variation trends across different cycles, indicating stable tool-soil interaction. Particle flow velocity was found to be synchronized and coordinated with force variations.

Combined with orthogonal experimental design and response surface analysis, the effects of tool camber, blade-inclined, and internal bending angle on the operating force and soil fragmentation rate were investigated. The operating effect was demonstrated by the regression model and significance analysis to be primarily determined by the tool camber angle and internal bending angle, while the resultant force and soil crushing rate variation were significantly influenced by their interaction.

Through parameter optimization, the optimal combination of three key parameters was determined: an 8.06° camber angle, 7.48° blade-inclined angle and 7.46° internal bending angle. Subsequent field validation tests demonstrated that the optimized tool achieved a cutting force of 2295.27 N and a soil fragmentation rate of 91.59%, both exceeding relevant national standards.

ACKNOWLEDGEMENT

This work was supported by National Key Research and Development Program of China (Project no. 2023YFD2001400), National Key R&D Program of China (Project no.2022YFE0125800).

REFERENCES

[1] Chang Y., Ge Y., Cao Z. (2025). Analysis of distribution characteristics and improvement practices of saline-alkali land in China (我国盐碱地分布特征及改良实践分析). *Journal of Agricultural Catastrophology*, 15(1), 244–246.

[2] Chen X., Chen L., Cai Z., Wang Q. (2025). Design and parameter optimization of a seed storage device of a wheat plot seeder (小麦小区播种机存种装置的设计与参数优化). *INMATEH - Agricultural Engineering*, 76(2), 121–130.

[3] Fang H., Ji C., Zhang Q., Guo J. (2016). Force analysis of rotary blade based on distinct element method (基于离散元法的旋耕刀受力分析). *Transactions of the Chinese Society of Agricultural Engineering*, 32(21), 54–59.

[4] Gao Z., Lu C., Wei X., Liu H., He J., Wang Q. (2023). Design and experiment of co-stirring combined corn strip straw cleaning device (协拨组合式玉米条带秸秆清理装置设计与试验). *Transactions of the Chinese Society for Agricultural Machinery*, 54(10), 68–79.

[5] Makange N., Ji C., Nyalala I. (2021). Prediction of precise subsoiling based on analytical method, discrete element simulation and experimental data from soil bin. *Scientific Reports*, 11(1), 11082.

[6] Popescu E., Nenciu F., Vlădut V. (2022). A new strategic approach used for the regeneration of soil fertility, in order to improve the productivity in ecological systems, *Scientific Papers. Series E. Land Reclamation, Earth Observation & Surveying, Environmental Engineering,* XI, 277–284.

[7] Qin K., Ding W., Fang Z., Du T., Zhao S., Wang Z. (2016). Design and experiment of ploughing and rotary tillage combined machine (犁翻旋耕复式作业耕整机的设计与试验). *Transactions of the Chinese Society of Agricultural Engineering*, 32(16), 7–16.

[8] Sun J., Wang Y., Ma Y., Tong J., Zhang Z. (2018). DEM simulation of bionic subsoilers (tillage depth > 40 cm) with drag reduction and lower soil disturbance characteristics. *Advances in Engineering Software*, 119(5), 30–37.

[9] Ucgul M., Saunders C. (2020). Simulation of tillage forces and furrow profile during soil-mouldboard plough interaction using discrete element modelling. *Biosystems Engineering*, 190, 58–70.

[10] Ucgul M., Saunders C., Fielke J.M. (2017). Discrete element modelling of top soil burial using a full-scale mouldboard plough under field conditions. *Biosystems Engineering*, 160, 140–153.

[11] Ucgul M., Saunders C., Li P., Lee S., Desbiolles J. (2018). Analyzing the mixing performance of a rotary spader using digital image processing and discrete element modelling (DEM). *Computers & Electronics in Agriculture*, 151, 1–10.

[12] Ungureanu N., Croitoru Şt., Biriş S., Voicu Gh., Vlăduţ V., Selvi K.Ç., Boruz S., Marin E., Matache M., Manea D., Constantin G., Ionescu M. (2015). Agricultural soil compaction under the action of agricultural machinery. *Proceedings of the 43rd International Symposium on Agricultural Engineering "Actual Tasks on Agricultural Engineering"*, 31–42, Opatija, Croaţia.

[13] Vlăduţ V., Gheorghe G., Marin E., Biriş S.Șt., Paraschiv G., Cujbescu D., Ungureanu N., Găgeanu I., Moise V., Boruz S. (2017). Kinetostatic analysis of the mechanism of deep loosening system of arable soil. *Proceedings of the 45th International Symposium on Agricultural Engineering "Actual Tasks on Agricultural Engineering"*, 217–228, Opatija, Croaţia.

[14] Vlăduţoiu L., Cârdei P., Vlăduţ V., Fechete L. (2017). Modern trends in designing and selecting the machine / equipment for soil deep tillage. 16th International Scientific Conference "Engineering for Rural Development", 1415–1420, Jelgava, Latvia.

[15] Wang D., Lu T., Zhao Z., Shang S., Zheng S., Liu J. (2024). Calibration of discrete element simulation parameters for cultivated soil layer in coastal saline alkali soil (滨海盐碱地耕作层土壤离散元仿真参数标定方法). *Transactions of the Chinese Society for Agricultural Machinery*, 55(11), 240–249.

[16] Wang Y., Rong G., Li H., Wang Q., He J., Lu C., (2019). Design and parameter optimization of vertical driving-type surface rotary tillage machine (立式驱动浅旋耙设计与参数优化). *Transactions of the Chinese Society of Agricultural Engineering*, 35(9), 38–47.

[17] Xiao W., Niu P., Wang P., Xie Y., Xia F. (2024). Simulation analysis and optimization of soil cutting of rotary blade by ANSYS/LS-DYNA (基于 ANSYS/LS-Dyna 旋耕刀切土仿真分析及优化). *INMATEH - Agricultural Engineering*, 72(1), 22–32.

[18] Yang Q., Lyu Z., Yan Y., Yang S., Li F., Song Z., Chen Y. (2025). Optimal design and experiment of vertical rotary harrow for mulberry plantation (桑园立式旋转动力耙优化设计与试验). *Transactions of the Chinese Society for Agricultural Machinery*, 56(1), 210–220.

[19] Zhang M., Wu C., Chen C. (2013). Drive system design and blade motion analysis of vertical rotary cultivator (立式旋耕机传动系统设计及旋刀运动分析). *Journal of Chinese Agricultural Mechanization*, 34(1), 66–69.

[20] Zhang S., Huang Y., Zhao H., Fu Z., Liu Z., Shi J. (2024). Design and experiment of cutting and throwing combined anti-blocking device for wide-seedbed seeding of wheat (切抛组合式小麦宽幅沟播破茬清秸防堵装置设计与试验). *Transactions of the Chinese Society for Agricultural Machinery*, 55(5), 40–52.